8-2013

Ultrasound-Intensified Mineral Carbonation

Rafael M. Santos
Katholieke Universiteit Leuven, rafael.santos@sheridancollege.ca

Davy Francois
Katholieke Universiteit Leuven

Gilles Mertens
Katholieke Universiteit Leuven

Jan Elsen
Katholieke Universiteit Leuven

Tom Van Gerven
Katholieke Universiteit Leuven

Accepted Manuscript

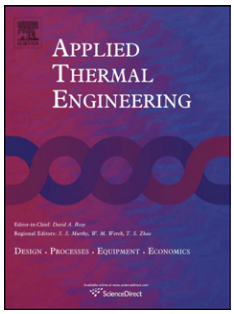

Ultrasound-intensified mineral Carbonation

Rafael M. Santos, Davy François, Gilles Mertens, Jan Elsen, Tom Van Gerven

PII: S1359-4311(12)00219-0

DOI: 10.1016/j.applthermaleng.2012.03.035

Reference: ATE 4096

To appear in: *Applied Thermal Engineering*

Received Date: 10 September 2011

Accepted Date: 21 March 2012

Please cite this article as: R.M. Santos, D. François, G. Mertens, J. Elsen, T. Van Gerven, Ultrasound-intensified mineral Carbonation, *Applied Thermal Engineering* (2012), doi: 10.1016/j.applthermaleng.2012.03.035.

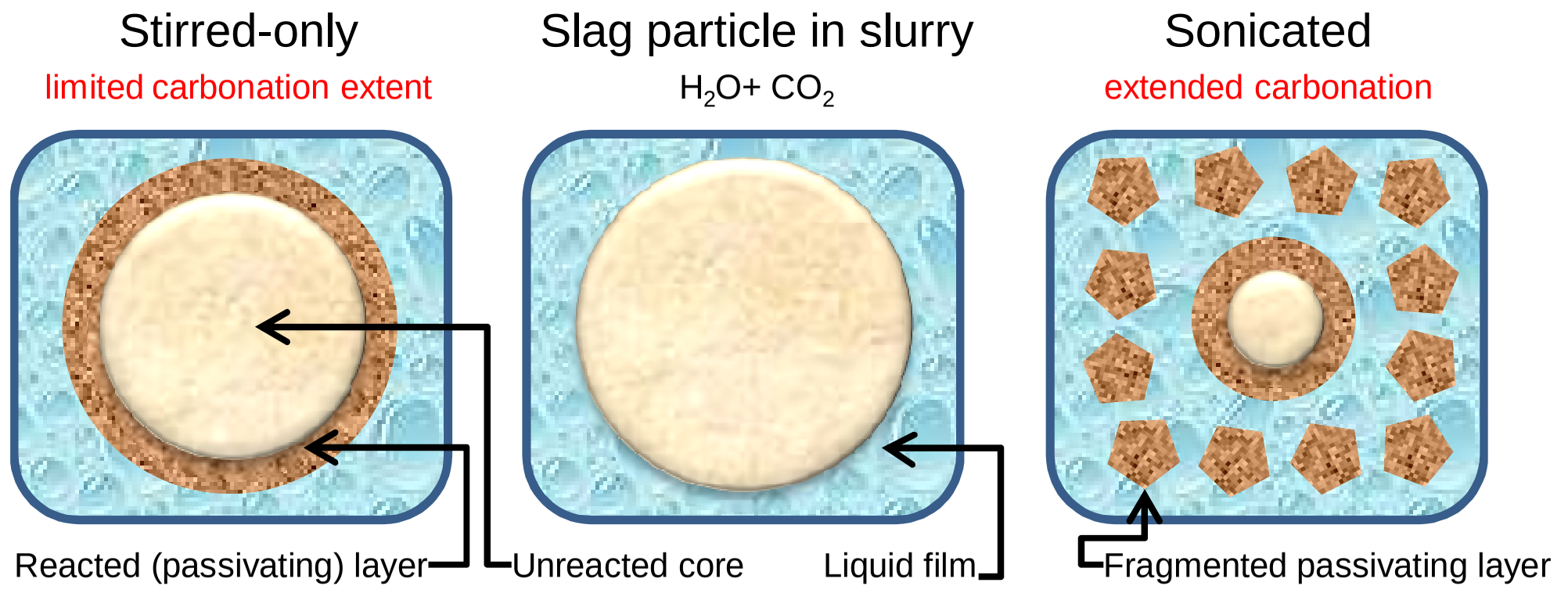
Stirred-only
limited carbonation extent
Slag particle in slurry
H_2O+ CO_2
Sonicated
extended carbonation
Reacted (passivating) layer
Unreacted core
Liquid film
Fragmented passivating layer

Ultrasound-Intensified Mineral Carbonation

Rafael M. Santos [a], Davy François [a], Gilles Mertens [b], Jan Elsen [b], Tom Van Gerven [a,*]

[a] Department of Chemical Engineering, Katholieke Universiteit Leuven, 3001 Heverlee, Belgium

[b] Department of Earth and Environmental Sciences, Katholieke Universiteit Leuven, 3001 Heverlee, Belgium

*Corresponding author. Tel.: +32 16 322342; Fax: +32 16 322991.

E-mail addresses: Rafael.Santos@cit.kuleuven.be (R.M. Santos),Tom.VanGerven@cit.kuleuven.be (T. Van Gerven)

ABSTRACT

Several aspects of ultrasound-assisted mineral carbonation were investigated in this work. The objectives were to intensify the CO_2 sequestration process to improve reaction kinetics and maximal conversion. Stainless steel slags, derived from the Argon Oxygen Decarburization (AOD) and Continuous Casting / Ladle Metallurgy (CC/LM) refining steps, were used for assessing the technical feasibility of this concept, as they are potential carbon sinks and can benefit from reduction in alkalinity (pH) by mineral carbonation. Ultrasound was applied by use of an ultrasound horn into the reaction slurry, where mineral carbonation reaction took place at 50 ^{o}C for up to four hours; comparison was made to solely mechanically mixed process. It was found that sonication increases the reaction rate after the initial stage, and permits achieving higher carbonate conversion and lower pH. AOD slag conversion increased from 30% to 49%, and pH decreased from 10.6 to 10.1; CC slag conversion increased from 61% to 73% and pH decreased from 10.8 to 9.9. The enhancement effect of ultrasound was attributed to the removal of passivating layers (precipitated calcium carbonate and depleted silica) that surround the unreacted particle core and inhibit mass transfer. Significant particle size reduction was observed for sonicated powders, compared to particle size growth in the case of stirring only; D[4,3] values increased without sonication by 74% and 50%, and decreased with sonication by 64% and 52%, respectively for AOD and CC slags. Considerations on scale-up of this technology, particularly with regards to energy efficiency, are also discussed.

Keywords: Mineral carbonation; Ultrasound; Process intensification; Stainless steel slag; Shrinking core; Carbon sink

1. Introduction

To overcome inefficiencies faced by current technologies and feasibility barriers that hinder the applicability of new technologies, process intensification (PI) promises to be a key facet of engineering development for years to come. Stankiewicz and Moulijn [1] defined PI as “any chemical engineering development that leads to a substantially smaller, cleaner, and more energy efficient technology”. Consequently, process intensification seeks to bring together fundamental aspects of process engineering technology (spatial, thermodynamic, functional, and temporal) and find the most optimum balance between them [2]. In particular, Reay [3] has identified that process intensification offers significant opportunities for reduction of greenhouse gas emissions. With this framework in place, an intensification route for mineral carbonation is explored herein.

Mineral carbonation involves the transformation or capture of carbon dioxide in a mineral form. The principal aims and advantages of this approach are the chemical stability and storage safety of mineral carbonates, the opportunities for process integration offered, and the potential for valorisation of otherwise low-value resources (virgin or waste) into useful products. The main barriers to its deployment in industry are: high energy intensity, slow reaction kinetics, low reaction conversion, complexities of the production chain and process adaptability, and competition for attention with alternative carbon capture technologies [4].

A potential intensification route for mineral carbonation involves the application of ultrasound as a source of focused energy capable of enhancing convective mass transfer, reducing diffusion barriers, activating precipitation sites and controlling crystal growth and morphology [4]. These aspects were studied in the present work in view of enhancing the carbonation of raw materials (calcium oxide) and alkaline waste materials (stainless steel slags), both with respect to conversion extent and pH stabilization.

2. Background

2.1 Mineral Carbonation

Mineral carbonation is the reaction of carbon dioxide with alkaline solids. It is a natural process in the global carbon cycle, producing carbonate minerals that are stable over geologic timescales, consequently having potential to sequester carbon dioxide in the effort to reduce greenhouse gas emissions and slow down climate change [5]. The reaction is also important for the production of solid particles in the paper, polymer, environmental protection and fertilizing industries [6,7]. Mineral carbonation can be performed with pure oxides (e.g. CaO, MgO), as well as virgin minerals (e.g. olivine $(Mg,Fe)_2SiO_4$, serpentine $Mg_3Si_2O_5(OH)_4$, wollastonite $CaSiO_3$) and alkaline waste materials (e.g. steel slags [7,8], incinerator and power plant fly ashes [9,10], paper mill waste [11], cement kiln dust [12], air pollution control residue [13], municipal waste incinerator bottom ash [14]). These waste materials can be used for carbonation due to the presence of alkaline oxides, hydroxides and silicates in their composition.

The carbonation process is an example of a gas-solid-liquid system and consists of several steps that can be illustrated in a simple system as follows:

1. Solvation: $CO_{2(g)} \Leftrightarrow CO_{2(l)}$
2. Reaction: $CO_{2(l)} + H_2O_{(l)} \Leftrightarrow H_2CO_{3(l)} \Leftrightarrow H^+ + HCO_3^- \Leftrightarrow 2H^+ + CO_3^{2-}$
3. Hydration: $CaO_{(s)} + H_2O_{(l)} \Leftrightarrow Ca(OH)_{2(s)}$
4. Ionization: $Ca(OH)_{2(s)} \Leftrightarrow Ca^{2+} + 2OH^-$
5. Precipitation: $Ca^{2+} + 2OH^- + 2H^+ + CO_3^{2-} \Rightarrow CaCO_{3(s)} + 2H_2O_{(l)}$

Kinetics of calcium carbonate precipitation in slurry can be approximated by a pseudo-second-order rate law of the form of Eq. (1) [15], where $Conv_{Ca}$ is the percent conversion of calcium from calcium-bearing minerals to calcium carbonate, t is reaction time, and k_p is the rate constant.

$$Conv_{Ca,t} = \frac{Conv_{Ca,\max} \times t}{\left(1/(k_p \times Conv_{Ca,\max})\right) + t} \quad (1)$$

A challenge of mineral carbonation reactions is the formation of an increasingly thick and dense carbonate layer surrounding the shrinking unreacted core of the solid particle [8]. This phenomenon, illustrated in Fig. 1, creates three rate limiting steps: (i) hydration of oxides/silicates; (ii) leaching of cations; and (iii) diffusion to reaction zone. The result is a limiting of the maximum calcium conversion to calcium carbonate ($Conv_{Ca,max}$, Eq. (1)), below 100%.

2.2 Ultrasound

To intensify the mineral carbonation process, in view of removing diffusion limiting layers and breaking particles, ultrasound was applied in this work. The use of ultrasound in chemical processes, also termed sonochemistry, applies sound waves in the range of 16 to 100 kHz, based on the premise that as frequency is lowered, the power delivered increases. Power is delivered to a solution by inducing cavitation, that is, the formation of small cavities or microbubbles that grow and collapse rapidly. Cavitation generates turbulence/circulation by acoustic streaming, producing fluid flow pattern similar to a jet loop reactor with higher axial velocities than radial velocities; these effects result in enhanced mixing and mass transfer, including dissolution of gases such as CO_2 [16]. The collapsing microbubbles produce high local temperatures, pressures and shear forces, including the formation of microjets. These effects cause solid surface erosion and interparticle collisions, leading to the removal of passivating layers or to the eventual breakage of particles [17].

Several methods exist to induce cavitation, the most common of which use: ultrasound horn, ultrasound bath, or hydrodynamic cavitation. The hydrodynamic method has been found more energy efficient and easier to scale up compared to horns and baths, of which the latter is reportedly more energy efficient due to greater irradiating surface area [18]. Conversely, acoustic equipment have been found to generate more intense/rigorous cavitation as indicated by greater collapse pressures ($O(10^7\text{-}10^8$ atm)) [18]. Gogate et al. [19] found, by use of a hydrophone to measure collapse pressure as a function of distance from an ultrasound horn tip, that the cavitational field is nonuniform, having spatial variation both in the axial and radial directions. Improvement of acoustic equipment efficiency has been suggested to be possible by geometric reactor configuration optimization, including use of multiple ultrasound transducers and combination of sonication and mechanical mixing [16]. Moreover, several process parameters are known to influence cavitation, both positively and negatively: for example, solids concentrations and gas sparging can contribute to generation of additional nuclei for cavitation, but also cause, respectively, cushioning effect resulting in decreased collapse pressure, and scattering of sound waves decreasing net energy delivery [20].

Ultrasound-mediated particle size reduction has been reported for powders of calcium carbonate [21], silica [22], clay [23], kaolinite [24], and aluminium oxide [25], and on activated sludge [26]. Experimental work is also reported on the use of an ultrasound horn to speed up carbonation and increase conversion. Nishida [27] tested the effect of sonication on the precipitation rate from a supersaturated solution of calcium and carbonate salts ($[Ca^{2+}] + [HCO_3^-]$), Ultrasonic irradiation, proportionally to ultrasound intensity and horn tip

diameter, was observed to accelerate the precipitation rate of calcium carbonate, which was optimized as a function of horn immersion depth. The physical mixing effect, macrostreaming, was suggested to cause the enhancement, more so than cavitation induced microstreaming. Morphology and size of calcium carbonate crystals were unaffected. Rao et al. [28] compared stirring versus horn ultrasonic slurry carbonation of fluidized bed combustion ashes. Conversions of CaO were reported to have increased from 23% to 62% at 15 minutes, and from 27% to 83% at 40 minutes. Particle size reduction achieved by sonication was attributed to cause the enhancement, allowing access to unreacted calcium oxide in the ash core. Sonawane et al. [29] passed CO_2 gas through a hole drilled along an ultrasound horn probe into a calcium hydroxide slurry, and found improved mixing and greater reduction of calcium carbonate particle size (from 104 nm to 35 nm), resulting from reduction in induction time (from 110 min to 20 min). López-Periago et al. [30] immersed an autoclave in a sonic bath to improve the carbonation of calcium hydroxide using supercritical carbon dioxide (13 MPa). The conversion to $CaCO_3$ after 60 minutes increased from 50 wt% without agitation, to 65 wt% with mechanical stirring, and 89 wt% with sonication.

2.3 Stainless Steel Slag

A class of waste materials that has good potential for implementation as a feed material for mineral carbonation is steel slags. Treatment and disposal of these slags can be a costly burden on steel plants. Sustainable solutions for the reuse of Argon Oxygen Decarburization (AOD) slag, generated in the stainless steel refining step, and Ladle Metallurgy / Continuous Casting (LM/CC) slag, produced during stainless steel casting, are still to be found. AOD slag exhibits a peculiar disintegration upon cooling due to the phase transformation of β-dicalcium silicate to the more stable, but less dense, γ-dicalcium silicate causing detrimental expansion forces in the material. The slag turns into a fine powder that causes severe dust issues during handling and storage in the steelworks; furthermore the slag in this form cannot be readily re-utilized or valorised, and often must be landfilled. One commonly used solution to avoid this problem is the incorporation of a small amount of doping agent (e.g. B^{3+}) in the crystal structure [31], which stabilizes the β-phase, producing a monolith product that has limited industrial application without further processing (e.g. crushing and milling). The boron addition also results in added processing cost and introduces environmental concerns regarding boron leaching. Furthermore, this methodology is not applied to CC slag due to process complexities, and the slag is disposed of in powder form by landfilling. More sustainable solutions leading to more useful products are desired. An integrated on-site mineral carbonation approach is envisaged as a

possibly economically favorable solution. Boron-free AOD and CC stainless steel slags (in powder form) were used for ultrasound-intensified mineral carbonation in this work.

Baciocchi et al. [32] studied the wet carbonation route of boron-free AOD slag (powder), and found maximum CO_2 uptake after 8 hours at 50 ^oC, 10 bar CO_2 and 0.4 liquid-to-solid (L/S) ratio. The CO_2 uptake of the aged slag, determined by calcimetry, was about 30 wt%, equivalent to 70% Ca conversion yield. Vandevelde [33] studied both boron-free AOD and CC slags (fresh powders) in wet carbonation at very mild conditions. Comparison of carbonation at 30 ^oC and 50 ^oC, 0.1 and 0.2 bar CO_2, and L/S varying from 0 to 0.5, allowed for determination of the optimum process conditions: 30 ^oC, 0.2 bar CO_2, L/S = 0.3. At these conditions, over 6 days, the CO_2 uptake of AOD and CC slags were 11 wt% and 15 wt% respectively, equivalent to 32% and 45% Ca-conversion respectively. Santos et al. [34] accelerated the process by performing slurry carbonation in a stirred autoclave (Buchi Ecoclave). Over 6 hours, at 60 ^oC and 3 bar CO_2, fresh AOD slag reaches 12 wt% CO_2 uptake (37% Ca-conversion) and fresh CC slag attains 17 wt% CO_2 (52% Ca-conversion).

3. Objectives

In view of the available literature on ultrasound-assisted mineral carbonation, the present study identified two main objectives for the intensification of mineral carbonation process:

1-) The effect of ultrasound in reduction of particle size of several powders ($Ca(OH)_2$, $CaCO_3$ and stainless steel slags) was investigated, to confirm the premise that ultrasound is capable of breaking particles and removing passivating layers, in view of permitting faster reaction and greater conversion during aqueous mineral carbonation.

2-) The effect of ultrasound on enhancing the carbonation kinetics and conversion of CaO, AOD and CC stainless steel slags was investigated by comparison of combined sonicated-stirred slurry process to stirred-only process. CO_2 uptake and pH reduction of carbonated materials were assessed.

4. Materials and Methods

For sonication an ultrasonic processor Hielscher UP200S was used, which operates at 24 kHz frequency. The probe used was an S14 sonotrode, which has a tip diameter of 14 mm, maximal amplitude of

125 µm, and an acoustic power density of 105 W/cm². A PT100 temperature sensor is also connected to the device. Experiments in slurry were conducted using a common glass beaker with a volume of two liters and diameter of approximately 14 cm; the beaker was filled with one liter of distilled water, which reached a height of 7.5 cm. Typical experiments were performed with 10 g of solids (this concentration was chosen to ensure that CO_2 solubility would not become a rate limiting factor under atmospheric conditions, as with higher solids loading the global rate of CO_2 uptake ($mmol_{CO2} \cdot l^{-1}$) would be higher, at least initially). The suspension was mixed solely with a mechanical stirrer (Heidolph type RZ-R1) and straight blade impeller at 340 rpm for stirred experiments, and in combination with the ultrasound horn during sonication experiments. Carbon dioxide gas was delivered to the solution from a compressed gas cylinder with flow controlled by a Brooks Sho-rate rotameter (R-2-15-AAA) and introduced into the slurry at 0.24 l/min using an aeration stone, which delivered finely dispersed gas bubbles. Temperature was controlled by use of a hot plate (IKAMAG RCT) for heating (in the case of stirred experiments) and water bath for cooling (in the case of sonicated experiments, since ultrasound produces heat, which must be dissipated to maintain a constant temperature). A temperature of 50 ^{o}C was maintained for carbonation experiments.

The following analytical grade materials were used in this study: CaO, $Ca(OH)_2$, $CaCO_3$ (Acros Organics), industrial grade CO_2 ≥99.5% (Praxair). Boron-free AOD and CC stainless steel slag powders were sieved to obtain the 63-200 µm fraction, which corresponded to 56% and 75% of the total slag masses respectively. This fraction was chosen as the fines (<63 µm) are less susceptible to the shrinking core barrier that hinders carbonation conversion, and the coarse fraction represents a small mass proportion (<6%) that is less susceptible to extensive carbonation. The chemical composition of the slags was determined by X-ray Fluorescence (XRF, Panalytical PW2400) and is presented in Table 1. It can be inferred from the calcium content of the slags that the maximum theoretical CO_2 uptake (mass fraction of calcium carbonate) of a fully carbonated specimen would be 30.9 wt% CO_2 for AOD slag, 29.0 wt% CO_2 for CC slag; in comparison pure CaO has a maximum uptake capacity of 44.0 wt% CO_2.

The mineral composition of the slags was determined by X-ray Diffraction (XRD, Philips PW1830) with peak analysis done in EVA (Bruker) software and mineral quantification performed using the Rietveld refinement method. Table 2 shows the interpreted mineral composition. The main mineral phase of both AOD and CC slags is gamma-dicalcium-silicate (γ-C_2S, Ca_2SiO_4), of which the latter contains significantly greater amount. AOD slag notably contains greater quantities of bredigite ($Ca_{14}Mg_2(SiO_4)_8$), cuspidine ($Ca_4Si_2O_7(F,OH)_2$), β-C_2S (Ca_2SiO_4), and åkermanite ($Ca_2MgSi_2O_7$), while CC slag possesses more periclase (MgO) and portlandite ($Ca(OH)_2$).

Particle size analysis of powder samples was determined by laser diffraction (Malvern Mastersizer). Morphological assessment was performed by imaging with a scanning electron microscope (SEM, Philips XL30 FEG). Carbonation efficiency was quantified by Thermal Gravimetrical Analysis (TGA, Thermo Scientific). An amount of 20-100 mg carbonated slag was weighed in a sample pan heated from 25 to 900 ^{o}C under a nitrogen atmosphere at a heating rate of 15 ^{o}C/min. The weight loss was recorded by the TGA microbalance and the amount of CO_2 uptake (wt%) was quantified by the ratio of weight loss between 500-800 ^{o}C (attributable to $CaCO_3$ decomposition to $CaO_{(s)}$ + $CO_{2(g)}$), over the carbonated sample mass at 500 ^{o}C (to eliminate any mass gain due to hydration/hydroxylation). Carbonation efficiency was defined as the ratio of actual CO_2 uptake over theoretical CO_2 uptake by the calcium content of the sample. Carbonation of the magnesium content of the slags was disregarded in the present study as the decomposition of magnesium carbonate at temperatures lower than 500 ^{o}C from TGA measurement is not clearly discernable, due to small conversions of MgO and Mg-silicates at the utilized process conditions, in agreement with results reported by Back et al. [35], and overlap with hydrates and meta-stable carbonates that may form during aqueous carbonation.

5. Results and Discussion

5.1 Optimization of Horn Sonication by Calorimetry

In order to optimally position the ultrasound horn in the present system (beaker with liquid slurry), in view of delivering constant, stable and maximal power sonication, experiments were performed to investigate the effect of probe depth and radial position. The ultrasound probe was immersed at several depths (defined as the distance from the probe tip to the air-water interface, ranging from 1 to 7 cm) into 1 liter water at the radial center position of the 2 liter volume beaker, and sonication was performed for 25 minutes. Similarly, to assess the effect of radial position, the probe was placed 2.5 cm from the beaker wall (compared to 7 cm in the case of centrally positioned probe), maintaining a depth of 2 cm for comparison. Sonication effect was measured by calorimetry, that is, the solution temperature increase over time. In this case the beaker was not immersed in the water bath, so that the temperature could rise freely (except for heat loss due to natural convection to the environment and conduction to the laboratory counter).

Fig. 2 presents calorimetry results as a function of probe tip position. A progressive increase in temperature change over time is seen as the depth increases from 1 cm to 5 cm. At 6 cm, a retardation

effect is seen, where the temperature takes longer to reach similar values as those for 4-5 cm. At 7 cm depth the temperature change is significantly hampered, indicating that the small distance of the tip to the beaker bottom (0.5 cm) is detrimental to sonication performance. The effect of radial position, on the other hand, is negligible: outer placement of the probe results only in a minor drop in temperature change. It is concluded from these results that a depth of 4.5 cm is optimal for the present system. The small effect of radial position signifies that co-placement of the ultrasound horn and mechanical mixer in the beaker, as done for the remaining experiments, has no detrimental effect on sonication performance.

Calorimetry results can also be used to estimate ultrasound efficiency, assuming temperature change is solely due to the implosion of cavitations generated by the probe (Table 3 shows that stirred unheated system does not yield significant temperature change). Using Eqs. 2 and 3, the thermal power delivered to the solution (P) and the ultrasound efficiency (η) can be determined. The temperature gradient is taken near the beginning of sonication to eliminate attenuation caused by heat loss to the environment. Using a temperature gradient of 11.5 ^{o}C during the first 400 s (Fig. 2, depth = 4 cm), or 0.02875 ^{o}C/s, the power delivered equals 120.2 W. Taking the net power of the ultrasound horn (Φ, calculated by Hielscher software based on gross electrical power consumed and resistance the probe experiences from the medium it is immersed in; i.e. in air equals zero) equal to 204.4 W (in the case of 0 g/l solids), the sonication efficiency equals 59%. In the presence of solids, the net power decreases, yet the temperature change and initial slope (not shown) remain the same. As a result, ultrasound efficiency increases to 72%. The decreased net power is evidence of the cushioning effect and scattering of sound waves described by Gogate et al. [19], while the increased efficiency agrees with their supposition that solids act as nuclei for cavitation formation, but could also be due to heat generation by interparticle attrition.

$$P = m \cdot c_p \cdot dT/dt \tag{2}$$

$$\eta = \frac{P}{\Phi} \tag{3}$$

5.2 Effect of Sonication on Particle Size

The carbonation reaction can be enhanced by the use of small particles which have a large surface to volume ratio. This large surface area enhances the hydration and dissolution rate of the calcium oxides and silicates and allows carbonate ions to react immediately without having to diffuse into the solid particle.

Sonication was tested as a means of reducing the particle size of four powder materials: AOD and CC slags, calcium hydroxide and ground calcium carbonate (sieved to <200 μm). Experiments were performed with 10 g of solids in 1 liter water, and ultrasound application for 30 minutes. The evolution of the volume-based particle size distributions by the use of ultrasound is shown in Fig. 3. The y-axis is plotted in unconventional logarithmic scale for easier visualization of the distribution shifts to smaller particle sizes.

Comparison of the AOD slag particle size distributions before (original) and after (US) sonication shows that ultrasound produces a significant amount of particles of a broad range below 15 μm; these small particles are likely a result of erosion of the original large particles in the size range 20-200 μm. In the case of CC slag, the particle size distribution appears to be unaffected by sonication. Different material mechanical properties such as hardness, toughness, brittleness and ductility, due to somewhat different chemical and mineralogical compositions may be responsible for this. Calcium hydroxide particle size distribution shifts significantly towards smaller values; as $Ca(OH)_2$ is a hydrated mineral, it can be subject to disordered crystal growth and agglomeration during fabrication, and thus it may be easily deagglomerated/fragmented by sonication, compared to dense slag particles. Ground calcium carbonate powder experiences substantial reduction in quantity of particles ranging from 40 to 150 μm, and a substantial increase in particles smaller than 40 μm; the perfect rhombohedral cleavage planes of calcite make it a favorable material for fragmentation by sonication/attrition. This result suggests that sonication can remove calcium carbonate layers that precipitate on the surface of slag particles during aqueous carbonation.

Table 4 presents the corresponding average particle sizes to the distributions in Fig. 3. Given are the volume mean diameter (D_{50}), the volume moment mean diameter (D[4,3]), and the surface area moment mean diameter (D[3,2]). The latter is particularly interesting for mineral carbonation as it relates to the active surface area of the material, which is primarily important for susceptibility towards carbonation. With the exception of $Ca(OH)_2$, the reduction in D[3,2] value surpasses those of the other two averages, indicating that particle surface erosion is the predominant consequence of sonication, as opposed to whole particle breakage. This furthermore emphasizes how sonication can be an ideal tool for reducing the rate/conversion limiting layers (carbonate and depleted silica) that form during mineral carbonation.

5.3 Effect of Sonication on Carbonation

Carbonation tests were conducted in slurries of CaO, AOD slag and CC slag using mechanical stirring alone and mechanical stirring combined with ultrasound (US). Process conditions were 10g solids in 1 liter solution at 50 ^{o}C. Carbonation tests were conducted for varying times, from 15 minutes to four hours to obtain information on carbonation kinetics and maximal achievable carbonation conversions. The comparison of sonication with mechanical stirring is made by quantifying the CO_2 uptake of the carbonated solids by thermogravimetric analysis (TGA), and expressing the results as percent calcium conversion to carbonate.

Fig. 4 presents carbonation data for the three materials tested. Data points are fitted to the pseudo-second order model equation (Eq. (1)), and corresponding coefficients are given in Table 5. For all three materials, sonicated carbonation achieves greater carbonation conversions as a function of time, particularly after 30 minutes of reaction, when the formation of rate-reducing carbonate and depleted-silica shells becomes more extensive. Maximal carbonation conversions with ultrasound are also higher for the three materials, an indication that sonication removes the conversion-limiting layers, permitting easier leaching of calcium ions from the unreacted particle core for reaction with carbonate ions. AOD carbonation conversion after four hours with sonication increased by 59%, from 30.5% to 48.5%; CC carbonation conversion, which were comparatively higher than AOD, likely as a result of more favorable mineralogy (e.g. greater γ-C_2S content), increased by a more modest 19%, from 61.6% to 73.2%. Maximal estimated conversions, described by the $Conv_{Ca,max}$ coefficients in Table 5, also follow similar trends.

In the case of CaO, carbonation was faster, with the ultrasound-intensified process reaching near completion (97.9%) after two hours, compared to 67.6% conversion with mechanical mixing alone. In the case of sonicated CaO carbonation, the kinetics trend no longer follows a pseudo second order model after one hour of carbonation, hence model coefficients were not calculated. For confirmation of suitability of the present process conditions (temperature, CO_2 flow rate, vessel geometry, and stirring speed) for studying carbonation kinetics and conversion, the carbonation rate of CaO during the first 30 minutes of reaction (when the reaction can be assumed to be driven solely by chemical kinetics and not impeded by mass transfer effects) was compared to values reported by Back et al. [35]. In the present work the initial carbonation rate, both with and without sonication, is calculated to be approximately 0.020 $mmol_{CO2} \cdot s^{-1} \cdot l^{-1}$, which matches the average carbonation rate over the initial 30 minutes reported by Back et al. [35] under similar process conditions.

The large content of alkaline minerals in stainless steel slags contributes to its high pH when in solution. High pH is an environmental hazard for slag disposal or reutilization, as it leads to leaching of several heavy

metals from the untreated slags (e.g. Cr, Cu, Mo, Ni, Pb, Zn). Carbonation has been shown to lead to reduction of pH and lowering of heavy metal leaching [34,36]. Fig. 5 (top) shows the effect of carbonation time on slurry pH of AOD and CC slags for the cases of sonication and mechanical mixing. Carbonated solids were filtered (589/3 filter paper) and oven dried at 105 ^{o}C for four hours; subsequently two grams of dried powder was added to 100 ml of ultra-pure water in a sealed bottle, agitated for two hours, and pH of the solution was measured. Original pH values of AOD and CC slags, prior to carbonation, were 11.4 and 12.3 respectively. For reactions executed for up to 60 minutes no difference in pH behavior is observed when comparing the cases with and without sonication; pH reduction of 0.3 and 0.9 units is obtained with carbonation of AOD and CC slags respectively. At two hours of reaction time, no further pH reduction is observed in the case of stirring, but significant pH drops are obtained with sonication: 0.5 and 1.5 pH units further reductions for AOD and CC slags respectively. At four hours, pH values drop for both stirring and sonication, but sonicated samples continue to exhibit significantly lower pH: a difference of 0.5 and 0.9 pH units for AOD and CC slags respectively. In fact, the pH of CC slag is identical to the theoretical pH value of pure $CaCO_3$ (9.91, unsaturated with respect to CO_2, Visual MINTEQ), and AOD slag is only slightly higher.

Plotting carbonation conversion versus pH (Fig. 5 bottom), it is possible to indirectly assess the effect of sonication on the removal of passivating layers. The removal of passivating layers would be expected, in theory and according to the shrinking core model, to expose the highly alkaline unreacted particle core to the solution, thereby maintaining the pH higher despite carbonation conversion. The results indicate that in the case of CC slag the calcium carbonate layer that forms on carbonated slag under mechanical mixing alone is not sufficient to completely shell the unreacted particle core, since the stirred and sonicated trends overlap. Furthermore, it demonstrates that the removal of the rate/conversion limiting layers (calcium carbonate and depleted silica) upon sonication is not necessarily detrimental to pH. At similar conversions (e.g. 50%) the pH of both stirred and sonicated samples are identical. In the case of AOD slag, it appears that the stirred carbonated slag reaches lower values of pH at lower carbonation conversion (30%), suggesting that its passivating layers are more effective in shielding the unreacted core. Nonetheless, the greater carbonation conversion achieved with sonication for the same carbonation times (2-4 hours) still demonstrate the benefit of utilizing sonication.

With a view of reducing ultrasound use, for energy conservation, it was tested whether reducing the ultrasound application time by one third could still produce as high levels of carbonation conversion, and as low pH values, as constant (100%) ultrasound application. Fig. 6 presents both sets of data for four cases: (i) mechanical stirring alone, (ii) mechanical stirring combined with 100% ultrasound application, (iii) mechanical

stirring combined with ultrasound application for 5 minutes every 15 minutes of reaction time (equivalent to 33% US application), and (iv) mechanical stirring combined with constant ultrasound application at 0.33 cycling (c) time (equivalent to 33% US application). Cycling refers to the fraction of experimental time during which sonication is applied, with sonication being pulsed on and off in short time intervals by an internal ultrasound horn setting. Carbonation experiments were conducted for two hours with CC slag. It can be seen from the figure that reducing ultrasound application leads to lower carbonation conversions than the constant US application case, but still better than mechanical stirring alone. Similarly, the pH values are higher when US application is decreased. In both instances, cycling US application over longer time periods (5/15 min) produced better results than the pulsed cycling (c = 0.33). It may be that the passivating layers are better removed by sonication when they acquire a certain minimum thickness, thereby being flaked off by cavitation implosions, microjects and interparticle collisions in near-micron-sized pieces. This would signify that prolonged, more thorough cleansing of the carbonated particle surface is more beneficial than more frequent but less efficient refreshment of the surface.

The effect of sonication on passivating layer removal from the surface of carbonated slag particles was further elucidated by measurement of particle size distributions and imaging of particle morphology. Fig. 7 shows volume-based particle size distributions of AOD and CC slag before carbonation (original) and after four hours of carbonation with (US) and without (stirred) sonication. For both slags similar shifts in particle size distributions take place. With stirring, the particle size distributions shift to larger particles; in fact not only does it appear that large (10-100 μm) particles grow, it also appears that the amount of particles smaller than 10 μm decreases significantly, signifying that agglomeration/joining of carbonated particles takes place. In the case of sonication, the effect is opposite: particle size distributions shift to smaller sizes, with clearly distinguishable creation of particles in the 0.2-1 μm and 2-10 μm ranges, and reduction in the fraction greater than 10 μm. It can be theorized that the smallest particles (0.2-1 μm) are formed by flaking of passivating layers, and the second mode (2-10 μm) is formed by fragmentation of slag particles and/or are the eroded remains of once larger slag particles.

Fig. 8 presents the average particles sizes of slag samples before and after carbonation as a function of reaction time. In the case of AOD slag under stirred carbonation, average particle sizes significantly increase after already 30 minutes of carbonation; only D[3,2] increases further with reaction time. This is in line with the fact that AOD carbonation with stirring reaches nearly maximum conversion in the first 30 minutes (Fig. 4); afterwards increase in D[3,2] likely signifies aggregation of smaller particles with the larger ones. With sonication, however, average particle sizes progressively decrease as a function of time, indicating the

continuing effect of ultrasound abrasion/milling. In the case of CC slag carbonation, average particle sizes progressively decrease and increase with and without sonication, respectively. It is interesting to note that CC particle size already clearly reduces after only 30 minutes of sonicated carbonation, when in the case of non-reacting sonication the particle size did not change (Table 4). This is suggestive that sonication not only removes the precipitated calcium carbonate layer, but also the depleted silica layer that once constituted the original slag particle material, and that this depleted silica layer is weaker than the original silicate material.

The morphology of CC slag particles prior and subsequent to carbonation is illustrated in Fig. 9. As already indicated by particle size distributions, a clear distinction is seen between stirred and sonicated carbonation, and in relation to the original uncarbonated sample. In the case of stirred carbonation, the absence of particles smaller than 20 μm is confirmed, and the envelopment of slag particles in thick calcium carbonate layers, composed of rhombohedral calcite crystals, is validated. On the other hand, the sample subjected to sonicated carbonation exhibits distinguishably different morphology, being composed mainly of much smaller particles. Two modes are visible, in agreement with laser diffraction results: flaky sub-micron particles, and rounded particle roughly 2-10 μm in size. It would appear that these rounded particles are remnants of larger particles that have been significantly eroded over time and/or particles whose rugged corners have been polished by sonication. These results substantiate the supposition that ultrasound is capable of removal of passivating layers and exposure of unreacted particle core to the reacting solution, overcoming the rate/conversion limiting shrinking core phenomenon and contributing to the intensification of the mineral carbonation reaction.

5.4 Energy Efficiency and Scale-up Considerations

In the present work, the process conditions utilized are not optimized for scaled-up application; they are meant to provide proof-of-concept. In particular, the power consumption of the ultrasound horn is unfeasibly high compared to the CO_2 capture obtained. For instance, taking the gross power consumption figure of 200 W, and two hours reaction time, the energy consumption of the process is 0.4 kWh. Using the average CO_2 emissions intensity for electricity generation in Belgium in 2009 of 198 gCO_2/kWh [37], CO_2 emissions of the ultrasound-intensified mineral carbonation process would be 79.2 grams. In comparison, the CO_2 uptake of CC slag under the present process conditions is only 2.3 grams per 10 g slag. It should be noted, however, that mineral carbonation of stainless steel slags is not meant only as a method for carbon capture, it is also a waste treatment solution, and potentially even a waste-to-product valorisation route. Taking the

electricity price for industrial consumers in Belgium of 10 Euro cents per kilowatt-hour [38], the treatment cost per tonne of slag would be 4000 Euros; also as unfeasibly high as the CO_2 emissions. Essentially these calculations suggest two orders of magnitude reduction are needed; i.e. if the CO_2 emissions were 0.8 grams per 10 g slag (giving 65% CO_2 capture efficiency) and treatment cost 40 Euros per tonne, the process would be industrially interesting.

There are several approaches to improve the feasibility of the process. First, the use of renewable electricity could make the CO_2 balance much more favorable. The Belgian electricity production sector is composed of a mix of nuclear (55%) gas (30%) and coal (10%), with minor contributions from wind and renewables [37]. These energy sources are notorious high CO_2 emitters (nuclear = 65 gCO_2/kWh, fossil fuels = 600-1200 gCO_2/kWh), compared to wind energy for example (15-25 gCO_2/kWh) [39]. This approach is only valid, however, if the captured CO_2 emissions originate from processes that cannot avoid CO_2 production (such as solid waste incineration, cement and steel production), rather than to curb CO_2 derived from fossil fuel power plants (in which case replacing fossil fuel based processes with renewable ones would be more efficient). Second, electricity prices are market dependant, with certain countries and jurisdictions charging less than half the price in Belgium. Third, the solids concentration in solution could be increased from 10 g/l to more typical values used in industrial slurry processes around 100-300 g/l. However, increasing solids concentration may cause the soluble concentration of CO_2 to be a rate limiting factor, thus increasing reaction time. As a response, it may be necessary to operate the process at higher CO_2 partial pressure, and utilize a combination of temperature and pH buffering that maximize dissociation of carbonic acid to carbonate ions, while still being favorable for calcium carbonate precipitation. A fourth approach, and perhaps most important, is optimization of ultrasound use, or utilization of other cavitation generating technologies. As Gogate et al. [18] suggested, hydrodynamic cavitation generation can be significantly more energy efficient than ultrasound horn (60% vs. <10% respectively); one note is that this study was conducted with the model reaction of decomposition of potassium iodide; efficiency results may differ when it comes to using ultrasound as an abrasion/milling mechanism. Moreover, Gogate et al. [16] have identified numerous parameters that should be considered for scale-up of ultrasound-assisted processes. These include ultrasound frequency (value and whether mono/multi/variable application), ultrasound probe dimensions (diameter and surface area, which affect US amplitude), liquid medium (e.g. additives that influence viscosity, vapor pressure and surface tension can be beneficial), and reactor configuration (flow geometry and ultrasound transducer placement). In summary they state that the “development of continuous reactors with tubular or hexagonal geometry is key to effective large scale operation, and use of multiple transducers

with a possibility of multiple frequency operation is recommended to get required cavitational effects while also minimizing the required energy consumption."

The combination of all these factors may allow ultrasound-intensified mineral carbonation to become an industrially feasible technology. Further work to meet these goals is intended by this research group. Moreover, with proof-of-concept confirmation on the application of ultrasound for overcoming the shrinking core barrier of liquid-solid processes, the approach utilized here can be extended to other chemical reactions that require intensification. In those cases, more favorable process conditions (e.g. material properties, reaction kinetics, required intensification extent) and economical incentives (e.g. product value, high cost competing technology) may permit more immediate application of this technology.

6. Conclusions

Ultrasound has been proven to be a potentially useful tool for intensification of mineral carbonation processes. Due to enhanced mixing, particle breakage and removal of passivating layers it was possible to accelerate the reaction kinetics, and achieve greater carbonation extent in shorter times and greater maximal conversion. The ultrasound enhancement mechanism has been attributed to the removal of the precipitated calcium carbonate and depleted silica layers that surround the carbonated particle and contribute to rate/conversion limiting effect due to mass transfer inhibition, thereby exposing the unreacted particle core to the reacting solution. These effects were evidenced in the present work by analysis of particle size distributions (via laser diffraction) and particle morphology (via scanning electron microscopy). When applied to argon oxygen decarburization (AOD) and continuous casting / ladle metallurgy (CC/LM) stainless steel slags, which are problematic waste materials posing environmental threat due to high alkalinity and heavy metal leaching potential, resulting in expensive disposal costs, ultrasound-intensified mineral carbonation has the potential to stabilize the materials and turn them into carbon sinks. It was found in the present work that sonicated carbonation resulted in significantly lower pH values of the carbonated materials, approaching the theoretical pH value of pure calcium carbonate, which should reduce their heavy metal leaching potential.

Acknowledgements

The K.U.Leuven Industrial Research Fund (IOF) is gratefully acknowledged for funding the Knowledge Platform on Sustainable Materialization of Residues from Thermal Processes into Products (SMaRT-Pro²) in which this work was performed. R.M.S is thankful for the PGS-D support from the Natural Sciences and Engineering Research Council of Canada (NSERC). The K.U. Leuven Department of Metallurgy and Materials Engineering are acknowledged for the use of XRF and SEM equipment.

REFERENCES

1 A.I. Stankiewicz, J.A. Moulijn, Process Intensification: Transforming Chemical Engineering. Chemical Engineering Progress 96 (2000) 22–34.

2 T. Van Gerven, A. Stankiewicz, Structure, Energy, Synergy, Time - The Fundamentals of Process Intensification. Industrial & Engineering Chemistry Research 48 (2009) 2465–2474.

3 D. Reay, The role of process intensification in cutting greenhouse gas emissions. Applied Thermal Engineering 28 (2008) 2011–2019.

4 R.M. Santos, T. Van Gerven, Process Intensification Routes for Mineral Carbonation. Greenhouse Gases: Science and Technology 1 (2011) 287–293.

5 K.S. Lackner, D.P. Butt, C.H. Wendt, Progress on binding CO_2 in mineral substrates. Energy Conversion and Management 38 (1997) S259–S264.

6 F.W. Tegethoff, J. Rohleder, E. Kroker, Calcium carbonate: from the Cretaceous period into the 21st century. Birkhauser Verlag, Basel, 2001.

7 S. Eloneva, A. Said, C.-J. Fogelholm, R. Zevenhoven, Preliminary assessment of a method utilizing carbon dioxide and steelmaking slags to produce precipitated calcium carbonate, Applied Energy (2011) 329–334.

8 W.J.J. Huijgen, G.-J. Witkamp, R.N.J. Comans, Mineral CO_2 Sequestration by Steel Slag Carbonation. Environmental Science & Technology 39 (2005) 9676–9682.

9 X. Li, M.F. Bertos, C.D. Hills, P.J. Carey, S. Simon, Accelerated carbonation of municipal solid waste incineration fly ashes. Waste Management 27 (2007) 1200–1206.

10 G. Montes-Hernandez, R. Pérez-López, F. Renard, J.M. Nieto, L. Charlet, Mineral sequestration of CO_2 by aqueous carbonation of coal combustion fly-ash. Journal of Hazardous Materials 161 (2009) 1347–1354.

11 R. Pérez-López, G. Montes-Hernandez, J.M. Nieto, F. Renard, L. Charlet, Carbonation of alkaline paper mill waste to reduce CO_2 greenhouse gas emissions into the atmosphere. Applied Geochemistry 23

(2008) 2292–2300.

12 D.N. Huntzinger, J.S. Gierke, L.L. Sutter, S.K. Kawatra, T.C. Eisele, Mineral carbonation for carbon sequestration in cement kiln dust from waste piles. Journal of Hazardous Materials 168 (2009) 31–37.

13 V. Prigiobbe, A. Polettini, R. Baciocchi, Gas–solid carbonation kinetics of Air Pollution Control residues for CO_2 storage. Chemical Engineering Journal 148 (2009) 270–278.

14 T. Van Gerven, E. Van Keer, S. Arickx, M. Jaspers, G. Wauters, C. Vandecasteele, Carbonation of MSWI-bottom ash to decrease heavy metal leaching, in view of recycling. Waste Management 25 (2005) 291–300.

15 G. Montes-Hernandez, F. Renard, N. Geoffroy, L. Charlet, J. Pironon, Calcite precipitation from CO_2–H_2O–$Ca(OH)_2$ slurry under high pressure of CO_2. Journal of Crystal Growth 308 (2007) 228–236.

16 P.R. Gogate, V.S. Sutkar, A.B. Pandit, Sonochemical reactors: Important design and scale up considerations with a special emphasis on heterogeneous systems. Chemical Engineering Journal 166 (2011) 1066–1082.

17 R.M. Wagterveld, L. Boels, M.J. Mayer, G.J. Witkamp, Visualization of acoustic cavitation effects on suspended calcite crystals. Ultrasonics Sonochemistry 18 (2011) 216–225.

18 P.R. Gogate, I.Z. Shirgaonkar, M. Sivakumar, P. Senthilkumar, N.P. Vichare, A.B. Pandit, Cavitation Reactors: Efficiency Assessment Using a Model Reaction. AIChE Journal 47 (2001) 2526–2538.

19 P.R. Gogate, P.A. Tatake, P.M. Kanthale, A.B. Pandit, Mapping of Sonochemical Reactors: Review, Analysis, and Experimental Verification. AIChE Journal 48 (2002) 1542–1560.

20 P.R. Gogate, A.B. Pandit, Sonochemical reactors: scale up aspects. Ultrasonics Sonochemistry 11 (2004) 105–117.

21 R. Isopescu, M. Mocioi, M. Mihai, C. Mateescu, G. Dabija, Modification of precipitated calcium carbonate particle size distribution using ultrasound field. Revista de Chimie 58 (2007) 246–250.

22 Y. Lu, N. Riyanto, L.K. Weavers, Sonolysis of synthetic sediment particles: particle characteristics affecting particle dissolution and size reduction. Ultrasonics Sonochemistry 9 (2002) 181–188.

23 A.L. Poli, T. Batista, C.C. Schmitt, F. Gessner, M.G. Neumann, Effect of sonication on the particle size of montmorillonite clays. Journal of Colloid and Interface Science 325 (2008) 386–390.

24 F. Franco, L.A. Pérez-Maqueda, J.L. Pérez-Rodríguez, The effect of ultrasound on the particle size and structural disorder of a well-ordered kaolinite. Journal of Colloid and Interface Science 274 (2004) 107–117.

25 V. Raman, A. Abbas, Experimental investigations on ultrasound mediated particle breakage. Ultrasonics

Sonochemistry 15 (2008) 55–64.

26 R.O. King, C.F. Forstert, Effects of sonication on activated sludge. Enzyme and Microbial Technology 12 (1990) 109–115.

27 I. Nishida, Precipitation of calcium carbonate by ultrasonic irradiation. Ultrasonics Sonochemistry 11 (2004) 423–428.

28 A. Rao, E.J. Anthony, L. Jia, A. Macchi, Carbonation of FBC ash by sonochemical treatment. Fuel 86 (2007) 2603–2615.

29 S.H. Sonawane, S.R. Shirsath, P.K. Khanna, S. Pawar, C.M. Mahajan, V. Paithankar, V. Shinde, C.V. Kapadnis, An innovative method for effective micro-mixing of CO_2 gas during synthesis of nano-calcite crystal using sonochemical carbonization. Chemical Engineering Journal 143 (2008) 308–313.

30 A.M. López-Periago, R. Pacciani, C. García-González, L.F. Vega, C. Domingo, A breakthrough technique for the preparation of high-yield precipitated calcium carbonate. The Journal of Supercritical Fluids 52 (2010) 298–305.

31 Y. Pontikes, P.T. Jones, D. Geysen, B. Blanpain, Options to prevent dicalcium silicate-driven disintegration of stainless steel slags. Archives of Metallurgy and Materials 55 (2010) 1167–1172.

32 R. Baciocchi, G. Costa, E. Di Bartolomeo, A. Polettini, R. Pomi, Carbonation of Stainless Steel Slag as a Process for CO_2 Storage and Slag Valorization. Waste and Biomass Valorization 1 (2010) 467–477.

33 E. Vandevelde, Mineral Carbonation of Stainless Steel Slag, Master's thesis, Katholieke Universiteit Leuven, Leuven, Belgium, 2010.

34 R.M. Santos, D. Ling, M. Guo, B. Blanpain, T. Van Gerven, Valorisation of thermal residues by intensified mineral carbonation, in: Proceedings of the 50th Conference of Metallurgists and the 6th International Symposium on Waste Recycling in Mineral and Metallurgical Industries (COM2011), Montreal, 2011, art.nr. 47189.

35 M. Back, M. Bauer, H. Stanjek, S. Peiffer, Sequestration of CO_2 after reaction with alkaline earth metal oxides CaO and MgO. Applied Geochemistry 26 (2011) 1097–1107.

36 R. Baciocchi, G. Costa, A. Polettini, R. Pomi, The influence of carbonation on major and trace elements leaching from various types of stainless steel slag, in: Proceedings of the Third International Conference on Accelerated Carbonation for Environmental and Materials Engineering (ACEME10), Turku, 2010, pp. 215–226.

37 Belgium Energy Efficiency Report, ABB. < http://www.abb.com > [accessed 04.09.11].

38 Europe's Energy Portal. <http://www.energy.eu> [accessed 04.09.11].

39 M. Lenzen, Life cycle energy and greenhouse gas emissions of nuclear energy: A review. Energy Conversion and Management 49 (2008) 2178–2199.

List of Figures

List of Tables

Table 1

Elemental composition of AOD and CC slags determined by XRF.

Elements (wt%)	Ca	Si	Mg	Cr	Al	Mn	Ti	Fe	S	V
AOD slag	40.6	15.2	4.2	0.53	0.53	0.33	0.21	0.17	0.16	0.02
CC slag	37.2	12.9	6.0	3.7	0.56	0.43	0.55	0.93	0.32	0.06

Table 2

Mineral composition of AOD and CC slags determined by XRD.

Mineral	Chemical formula	AOD slag	CC slag
γ-C_2S	Ca_2SiO_4	28.9	47.4
Bredigite	$Ca_{14}Mg_2(SiO_4)_8$	24.5	5.2
Cuspidine	$Ca_4Si_2O_7(F,OH)_2$	13.9	9.3
β-C_2S	Ca_2SiO_4	8.2	4.0
Merwinite	$Ca_3Mg(SiO_4)_2$	7.3	6.6
Periclase	MgO	6.2	15.5
Åkermanite	$Ca_2MgSi_2O_7$	2.8	0.5
Gehlenite	$Ca_2Al_2SiO_7$	2.7	1.1
Hibonite	$CaAl_{12}O_{19}$	2.5	2.8
Quartz	SiO_2	1.1	0.2
Portlandite	$Ca(OH)_2$	1.1	2.3
Magnetite	Fe_3O_4	0.5	3.4
Lime	CaO	0.3	-
Fayalite magnesian	$(Fe,Mg)_2SiO_4$	-	1.7

Table 3

Effect of solids content of sonicated (60 min) slurry on ultrasound net power delivered and calorimetry.

Mixing method	stirred	sonicated	sonicated	sonicated	sonicated
Solids content (g/l)	0	0	10	20	50
Avg. net power Φ (W)	-	204.4	173.1	166.9	166.8
ΔT (^{o}C)	0.6	39.9	40.6	40.1	40.1

Table 4

Average particle sizes of original and sonicated (30 min) powders of AOD and CC slags, $Ca(OH)_2$ and $CaCO_3$.

AOD slag (μm)				$Ca(OH)_2$ (μm)			
	Original	Sonicated	Reduction		Original	Sonicated	Reduction
D_{50}	52.5	41.1	-22%	D_{50}	29.7	5.2	-83%
D[4,3]	58.4	49.8	-15%	D[4,3]	60.7	43.2	-29%
D[3,2]	4.4	2.7	-39%	D[3,2]	1.8	0.9	-51%
CC slag (μm)				$CaCO_3$ (μm)			
	Original	Sonicated	Reduction		Original	Sonicated	Reduction
D_{50}	19.2	21.2	-	D_{50}	266.0	233.8	-12%
D[4,3]	33.0	35.4	-	D[4,3]	236.9	204.0	-14%
D[3,2]	2.6	2.5	-5%	D[3,2]	25.7	6.4	-75%

Table 5

Fitted pseudo-second order model (Eq. (1)) coefficients for stirred and sonicated carbonation of AOD and CC slags and CaO.

	AOD Stirred	AOD US	CC Stirred	CC US	CaO Stirred	CaO US
$Conv_{Ca,max}$	30.1%	58.0%	74.0%	85.3%	96.2%	*
k_p (min^{-1})	0.3715	0.0368	0.0279	0.0290	0.0211	*

* does not follow pseudo second order model

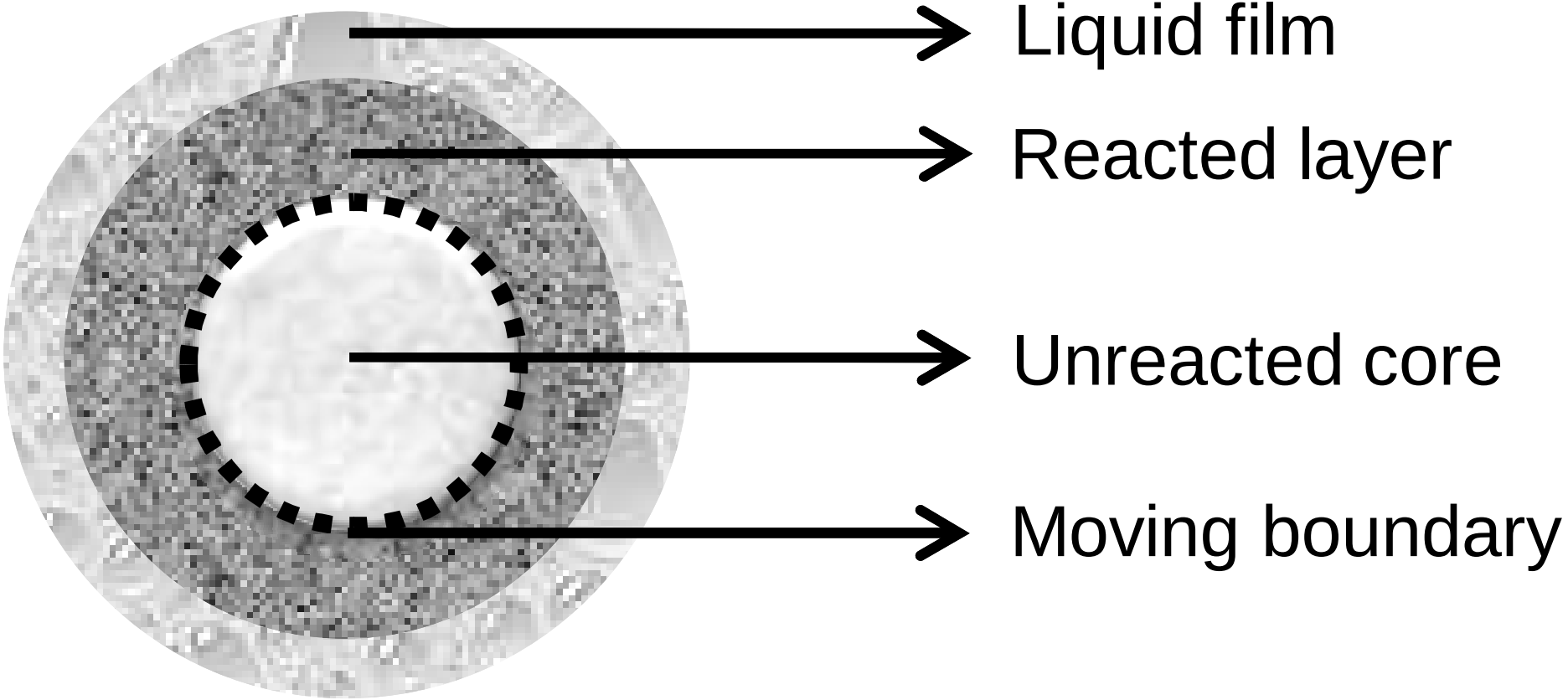
Liquid film
Reacted layer
Unreacted core
Moving boundary

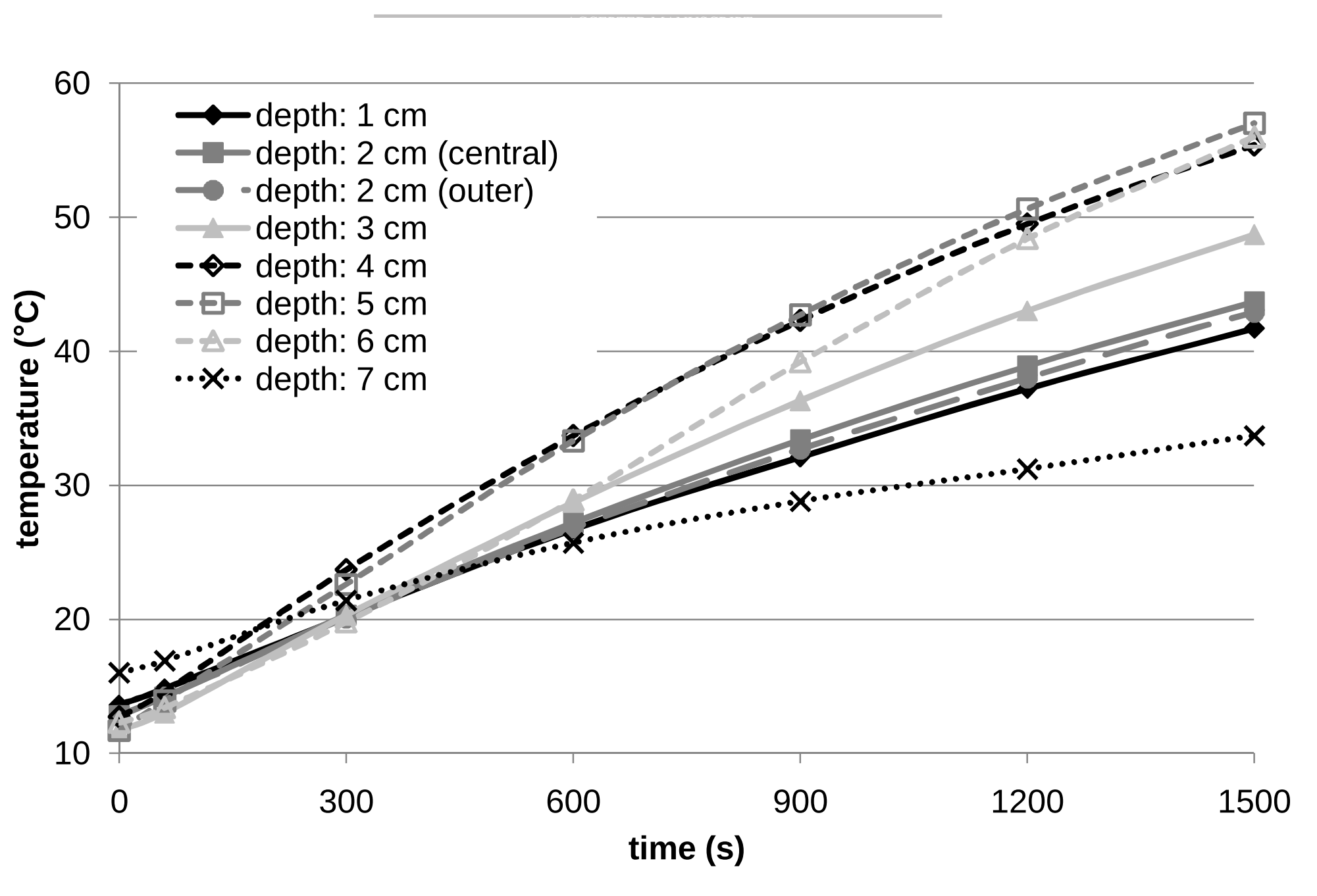
depth: 1 cm
depth: 2 cm (central)
depth: 2 cm (outer)
depth: 3 cm
depth: 4 cm
depth: 5 cm
depth: 6 cm
depth: 7 cm
temperature (°C)
60
50
40
30
20
10
0
300
600
900
1200
1500
time (s)

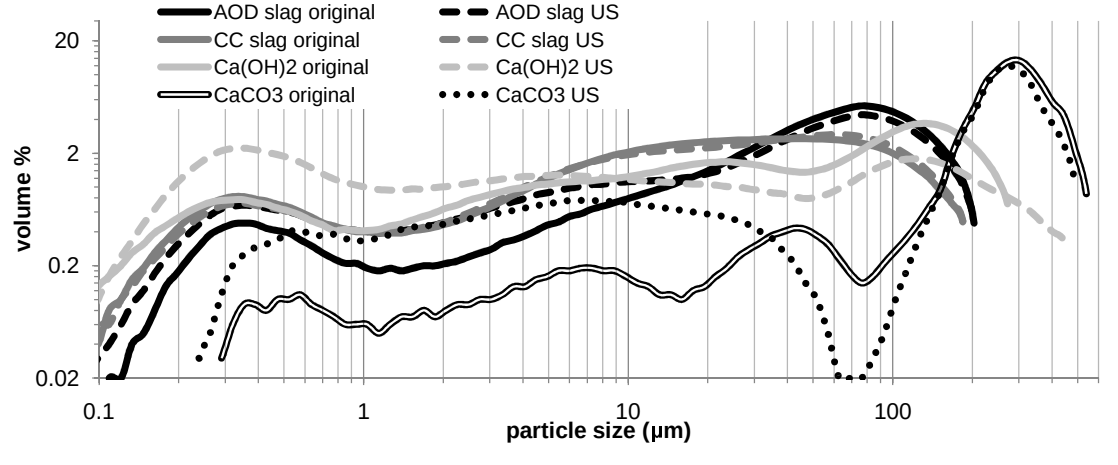

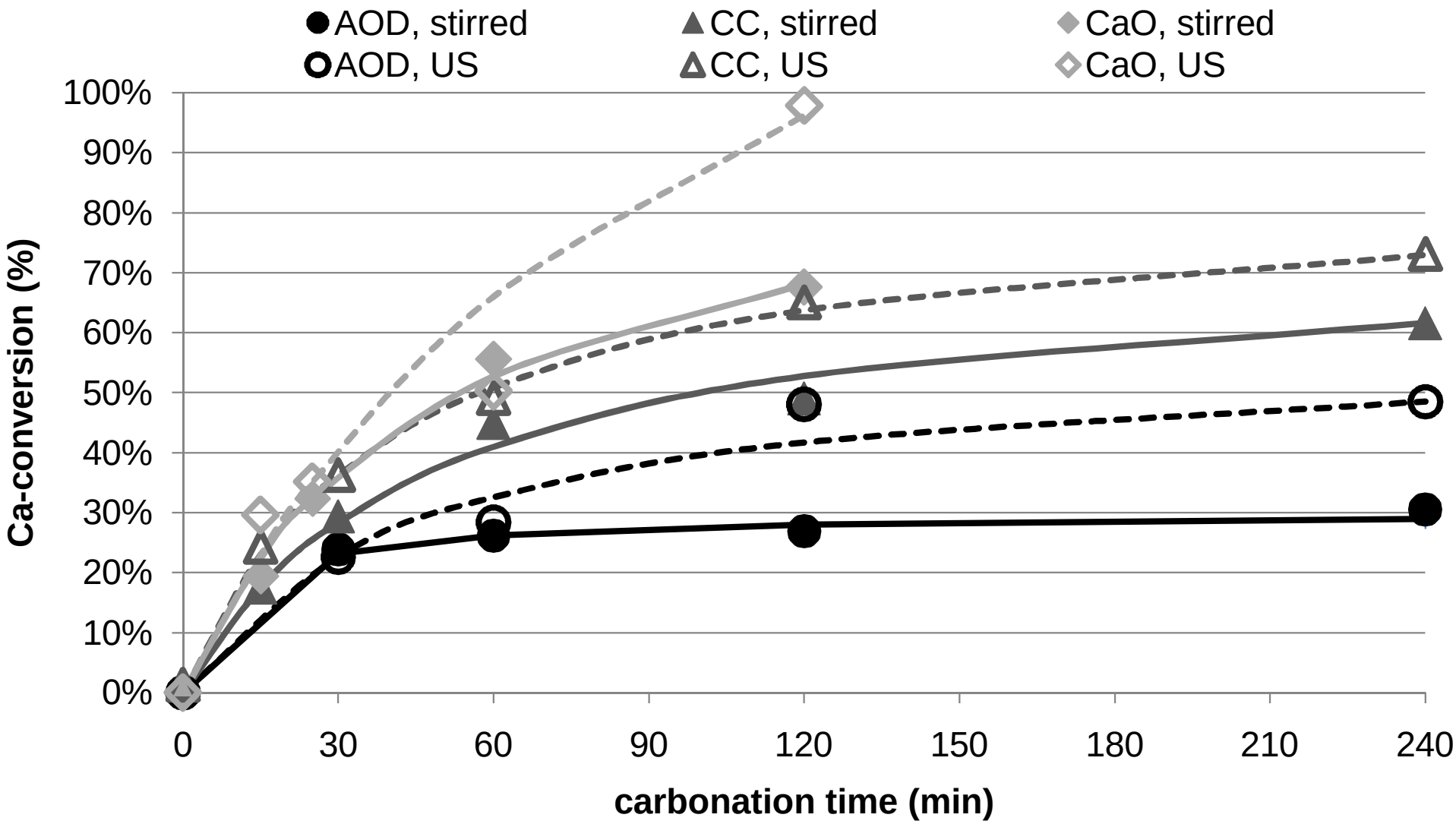

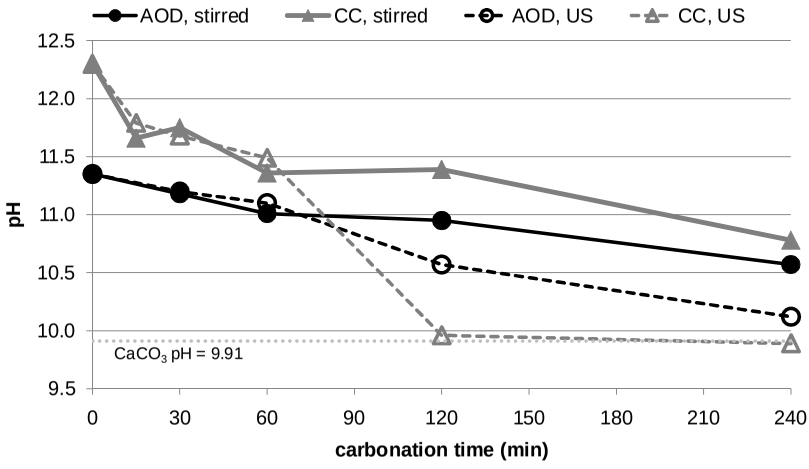
AOD, stirred
CC, stirred
AOD, US
CC, US
12.5
12.0
11.5
11.0
10.5
10.0
9.5
pH
CaCO3 pH = 9.91
0
30
60
90
120
150
180
210
240
carbonation time (min)

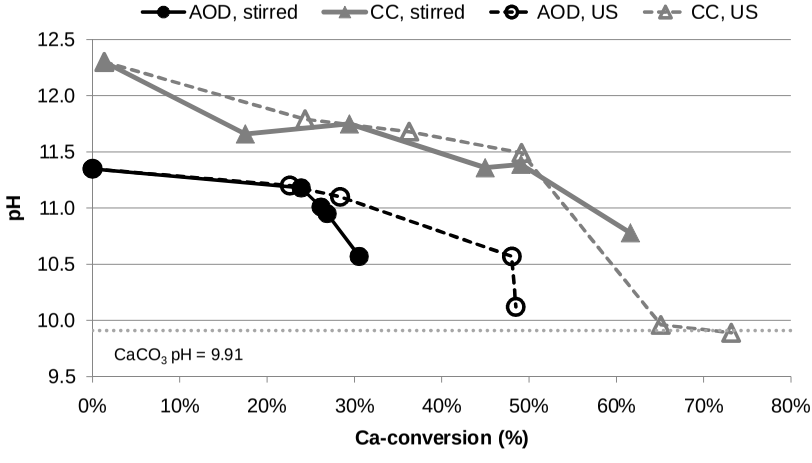
AOD, stirred
CC, stirred
AOD, US
CC, US
12.5
12.0
11.5
11.0
10.5
10.0
9.5
pH
CaCO3 pH = 9.91
0%
10%
20%
30%
40%
50%
60%
70%
80%
Ca-conversion (%)

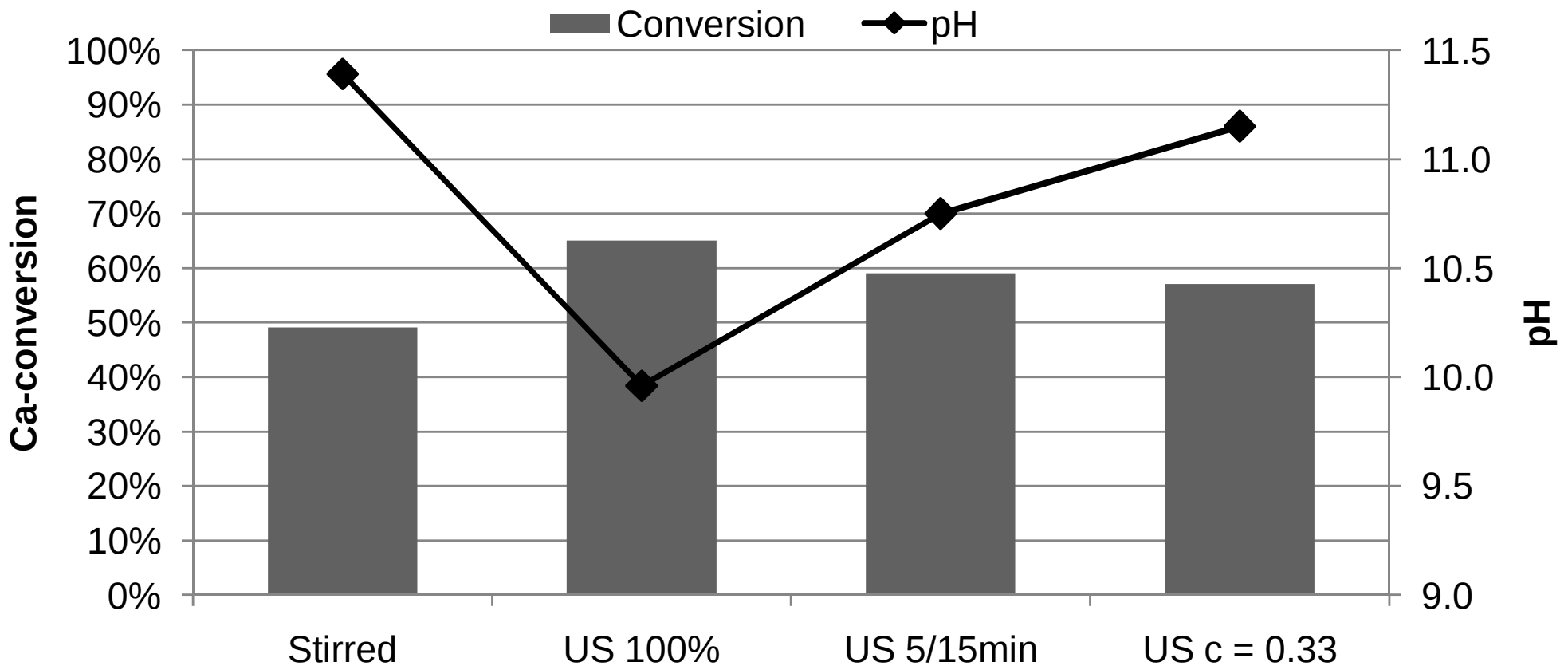

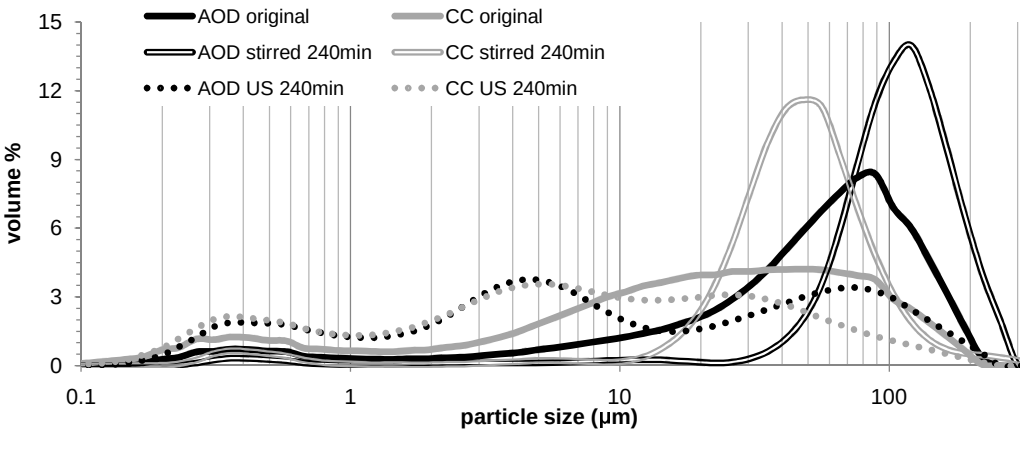

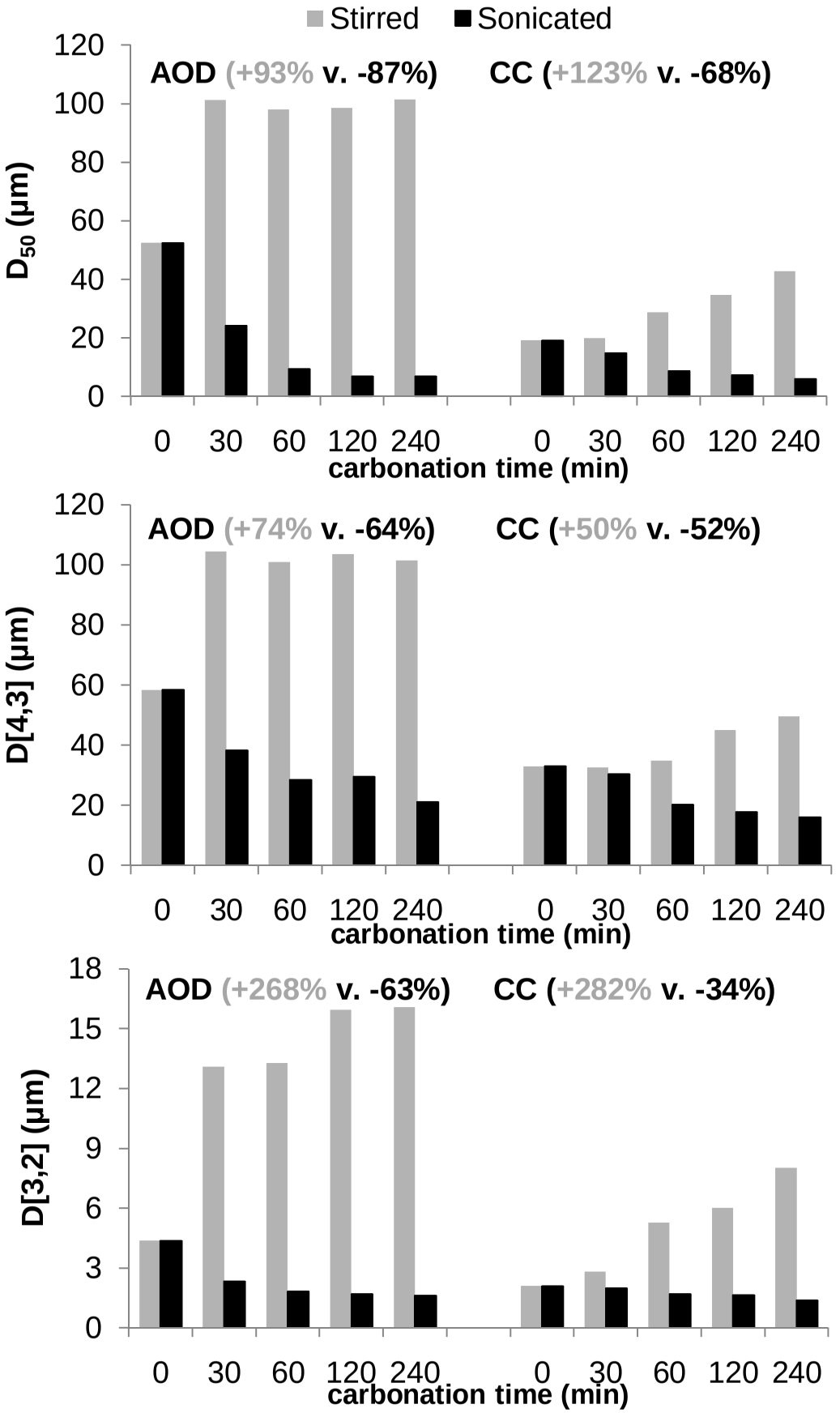
Stirred
Sonicated
AOD (+93% v. -87%)
CC (+123% v. -68%)
D50 (µm)
120
100
80
60
40
20
0
0 30 60 120 240 0 30 60 120 240
carbonation time (min)
AOD (+74% v. -64%)
CC (+50% v. -52%)
D[4,3] (µm)
120
100
80
60
40
20
0
0 30 60 120 240 0 30 60 120 240
carbonation time (min)
AOD (+268% v. -63%)
CC (+282% v. -34%)
D[3,2] (µm)
18
15
12
9
6
3
0
0 30 60 120 240 0 30 60 120 240
carbonation time (min)